Eur. Radiol. 9, 73–77 (1999)

European
Radiology

Original article

3D MR gastrography: exoscopic and endoscopic analysis of the stomach

M. R. Schmid[1], **T. F. Hany**[1], **L. Knesplova**[1], **R. Schlumpf**[2], **J. F. Debatin**[1]

[1] Institute of Diagnostic Radiology, University Hospital Zurich, Rämistrasse 100, CH-8091 Zurich, Switzerland
[2] Department of Surgery, University Hospital Zurich, Rämistrasse 100, CH-8091 Zurich, Switzerland

Received: 27 November 1998; Revision received: 23 February 1998; Accepted: 3 March 1998

Abstract. The aim of this study was to evaluate the feasibility of MR gastrography, based on 3D MRI following the oral administration of Gd-DOTA-enriched blueberry juice, in order to depict alterations of the gastric wall. The stomachs of three volunteers and three patients were examined on a 1.5-T MR system. Following ingestion of 400 ml of blueberry juice spiked with 2 ml of Gd-DOTA, each subject underwent 3D MR imaging in three positions: 45° left lateral decubitus, supine, and 45° right lateral decubitus. In each position, a coronal 3D SPGR acquisition consisting of 60 continuous 2-mm slices was acquired over a 35-s breathhold (TR/TE = 4.0/1.8 ms, 40° flip angle, 0.5 excitations, voxel size of 1.25 × 1.66 × 2.00 mm). Multiplanar reformats (MPR), maximum intensity projections (MIP), surface shaded displays (SSD), and virtual intraluminal endoscopic views (VIE) were calculated. Magnetic resonance gastroscopy was tolerated well by all subjects without adverse effects. Based on the 3D MRI data sets acquired in various patient positions, all regions of the stomach and the proximal duodenum were visualized to good advantage. Whereas MPR and MIP provided a morphologic overview, SSD and VIE images permitted analysis of the gastric mucosa. Normal mucosa could be differentiated from the course and irregular pattern characterizing carcinomatous infiltration. The 3D SPGR data sets acquired following ingestion of oral Gd-DOTA-spiked blueberry juice permits exoscopic and virtual endoscopic viewing of the stomach.

Key words: 3D MR imaging – Oral contrast agents – Gastric tumors

Introduction

Although the introduction of double-contrast radiographic techniques has reduced the comparative advantage of endoscopy over barium studies [1], most studies suggest that upper gastrointestinal (UGI) endoscopy is more accurate [2], particularly regarding the evaluation of bleeding lesions [3] and the post-operative stomach [4]. Thus, in most centers around the world the continued need for diagostic assessment of the stomach is met by UGI endoscopy [5].

Upper gastrointestinal endoscopy is a safe and effective diagnostic procedure. Complications do exist, however [6], and procedure-related costs are considerable [7]. Furthermore, direct endoscopic viewing of the gastric wall is not without its limitations. The endoscopic inspection is limited to visualization of the gastric mucosa. Disease processes affecting the gastric wall are only indirectly depicted [1]. Disease extension beyond the confines of the gastric wall as well as lymph node metastasis in the perigastric region are missed completely. These limitations underscore the desirability of an inexpensive technique which provides both endoscopic and exoscopic information.

The availability of high-performance gradient systems has allowed for the acquisition of complex 3D MRI data sets within the confines of a comfortable breathhold [8]. Based on the 3D nature or the MR data and the tremendous contrast between signal within the vascular lumen and surrounding structures, the data can be processed to provide virtual angioscopic images [9]. The same technique has already been applied to the colon [10, 11]. We now describe an adaptation of this technique to imaging of the stomach. In this preliminary study the technique was evaluated in three volunteers without any gastric symptomatology as well as three patients with known gastric pathologies. With the help of simple post-processing algorithms, the underlying MR data provides exoscopic as well as endoscopic views of the stomach.

Beyond describing the technique, the purpose of this study was to optimize 3D gastric MRI regarding patient positioning and data post-processing by analyzing the stomach of healthy volunteers and of patients with different gastric pathologies.

Correspondence to: M. R. Schmid

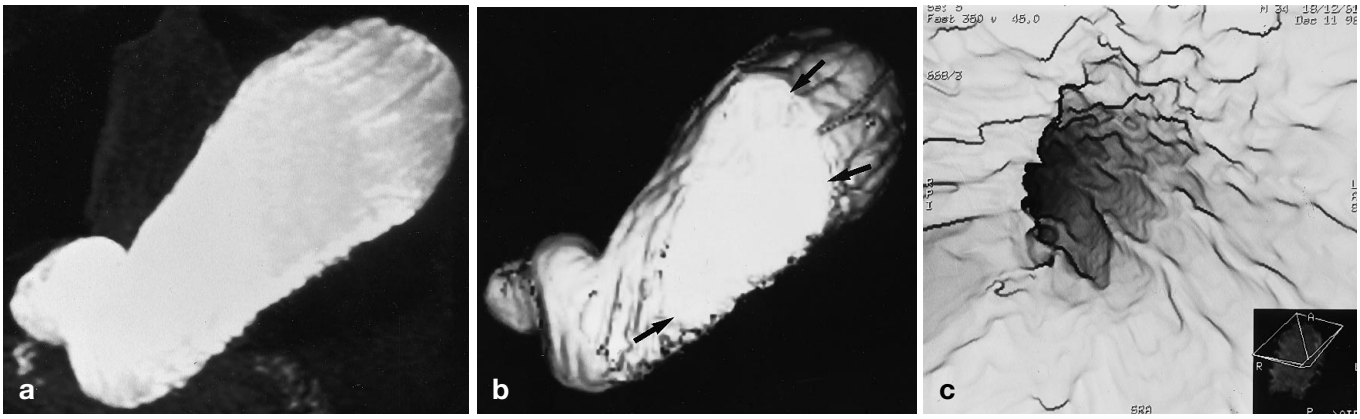

Fig. 1. Maximum intensity projection (MIP) image of a 3D data set depicting **a** a normal stomach acquired in the 45° left lateral decubitus position. The stomach is homogeneously filled with contrast, which has not spilled into the duodenum. Signal in the surrounding tissues is nulled reflecting the very short repetition time. The gastric contours are well appreciated. **b** Surface shaded display of the same normal stomach provides a more 3D appreciation of the gastric folds. Note the air–fluid level induced by residual air within the gastric lumen *(arrows)*. **c** Virtual intraluminal endoscopic image of the gastric fundus details the regular gastric folds from an internal perspective. Limitations in spatial resolution are clearly apparent

Subjects and methods

Patients and volunteers

After fasting for 4 h, three volunteers (27, 29, and 35 years old) without any gastric symptomatology (Fig. 1 a, b) and three patients (49, 58, and 80 years) were transferred to the MR suite for gastric MRI. Following gastric banding for morbid obesity, one patient (Fig. 2) had undergone a conventional single-contrast barium study 6 h preceding the MR exam. Upper GI endoscopy performed on the second patient 6 h prior to the MRI exam revealed a large polypoid mass (Fig. 3). Pathohistology demonstrated the mass to be a large gastric polyp with polypous gastric wall infiltration. The lesion in the gastric antrum of the third patient was discovered to be an adenocarcinoma.

Informed consent was obtained from all subjects in accordance with guidelines set forth by the hospital's internal review board.

The subjects were placed on the MRI table in a left decubitus position with their heads elevated. In this position they were asked to ingest 400 ml of blueberry juice spiked with 2 ml of Gd-DOTA (Dotarem, Guerbet Laboratories, Cedex, France) rendering a concentration of 25 μmol/ml. Preceding in vitro experiments had demonstrated this mixture to be characterized by T1 and T2 relaxation times of 32 ms and 8 ms, respectively. To reduce bowel motion, scopolamine (20 mg intravenously) was administered prior to the subject being placed on the MRI table.

Fig. 2. **a** Source image of a 3D gastric data set obtained in a 49-year-old woman (supine position) following gastric banding for morbid obesity. The stomach is filled with signal-rich contrast. **b** The proximal pouch is seen to even better advantage on the sagittal reformatted image of the same 3D data set. **c** Virtual intraluminal endoscopic view of the proximal pouch permits assessment of the gastric folds and depicts the residual lumen following the banding procedure *(arrow)*

MR imaging

Imaging was performed on a 1.5-T MRI scanner (Signa EchoSpeed, GE Medical Systems, Milwaukee, Wis.) equipped with an ultrafast three-axis gradient system characterized by a maximum amplitude of 22 mT/m, and a slew rate of 120 mT/m per millisecond. A

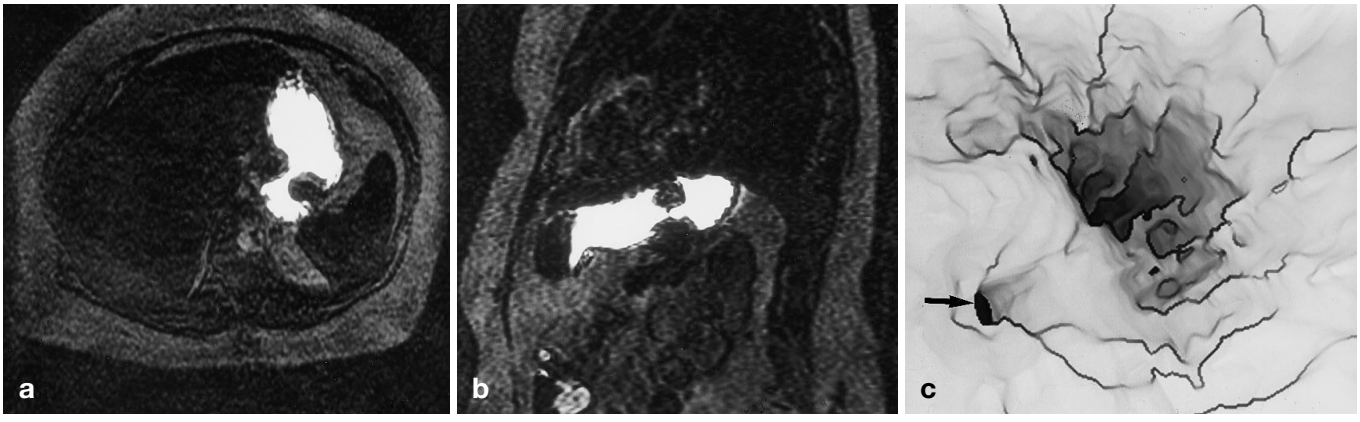

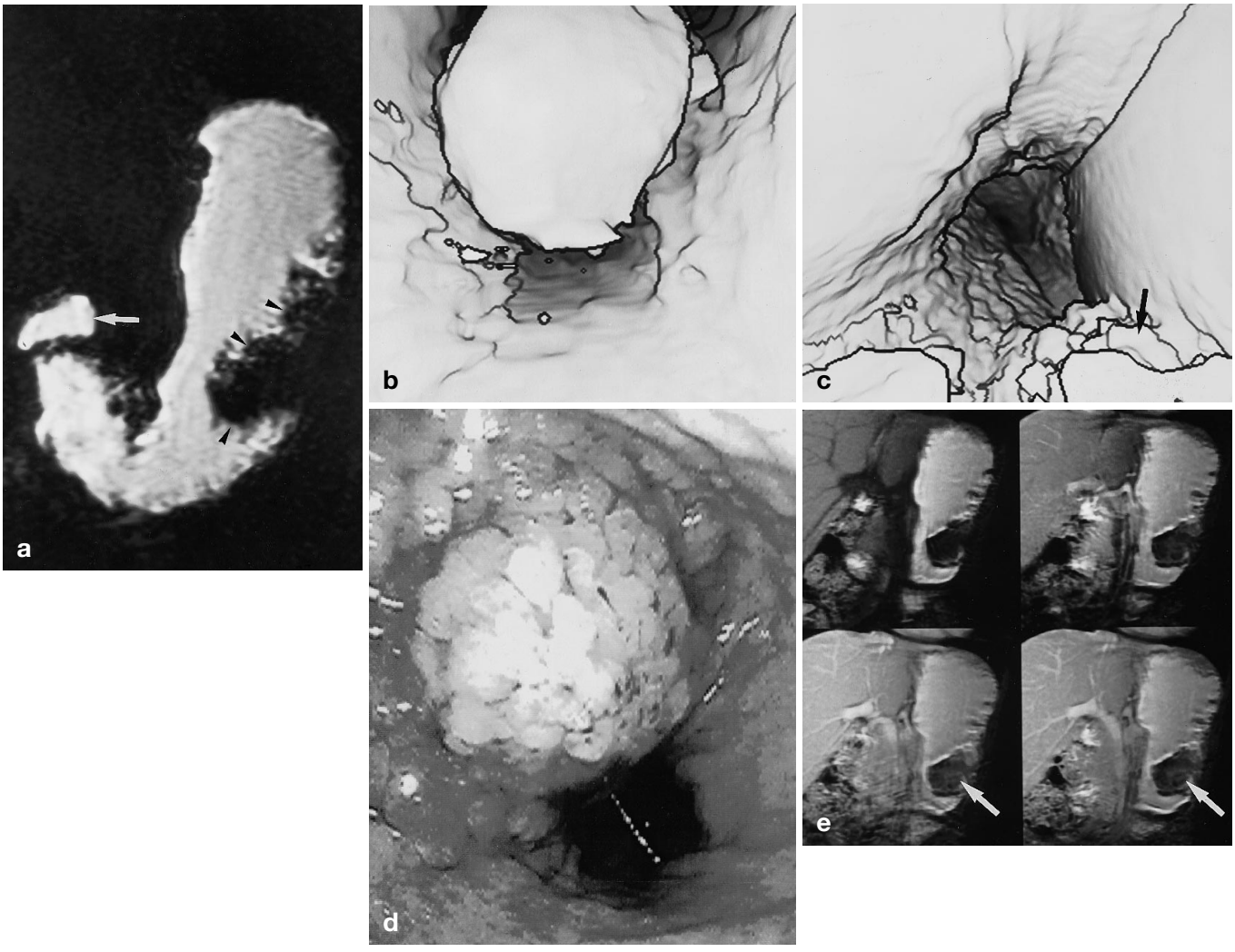

Fig. 3. **a** Maximum intensity projection image of the stomach in a 58-year-old man with a polypoid gastric mass *(arrowheads)*. The data were acquired breathheld in the supine position. The entire stomach as well as the duodenal bulb *(arrow)* are filled with contrast. **b** Virtual intraluminal endoscopic (VIE) view of the gastric mass as seen from the fundus. **c** Second VIE view of the gastric wall just beyond the polypoid mass looking toward the gastric antrum. The image reveals thickened and irregular gastric folds *(arrow)*. **d** Conventional gastroscopy confirmed the presence of the polypoid mass as well as fold thickening. **e** Gradient-recalled-echo images acquired prior to *(top left)*, as well as immediately *(top right)*, 1 min *(bottom left)* and 2 min *(bottom right)* following intravenous administration of paramagnetic contrast illustrates some *(arrows)* of the gastric mass

phased-array torso coil was used for signal transmission and reception using standard receivers.

Following ingestion of the contrast, the subjects were advanced into the bore of the scanner. Based on an axial localizing sequence, a 3D acquisition covering the stomach was planned. Repetition (TR) and echo times (TE) of the employed prototype 3D gradient-echo sequence with spoiling gradients [8] were 4.0 and 1.8 ms, respectively. Radio-frequency (RF) excitation was performed with a 3-kHz bandwidth. The sampling bandwidth was ± 62.5 kHz. The flip angle was 40°. A 32-cm field of view (FOV) coupled with a 256 × 192 matrix provided an in-plane resolution of 1.25 × 1.66 mm. Partial (half) k-space sampling in the phase-encoding direction permitted the acquisition of 64 contiguous 2-mm sections in 35 s; of these, 60 sections were reconstructed. To compensate for the presence of residual air in the stomach, the subjects were imaged in three positions: (a) left lateral decubitus with 45° body inclination to the left side; (b) supine with the back elevated (20°); and (c) right lateral decubitus with 45° body inclination to the right side

In each position, 3D SPGR data sets were acquired in the coronal plane.

Finally, to permit local and hepatic staging, a 2D multiplanar coronal acquisition (TR 150 ms, TE 2.1 ms, 60° flip angle) consisting of 20 contiguous 8-mm sections was obtained from the upper abdomen in the patient with the gastric mass (Fig. 3 d). Images were acquired prior to as well as immediately, 60 s and 120 s following intravenous administration of Gd-DTPA (Magnevist, Schering AG, Berlin, Germany) at a dose of 0.1 mmol/kg.

Image processing and analysis

The 3D data sets, which consisted of 60 contigeuous 2-mm sections, were post-processed on an Advantage Windows workstation (GE Medical Systems, Buc, France) running on the Solaris 2.3 operating system. The hardware platform consisted of a SPARC-20 workstation (Sun Microsystems, Mountain View, Calif.) with 128 Mbytes of main memory and 260 Mbytes of swap space. Maximum intensity projections (MIP) were acquired as well as shaded surface displays (SSD) of the contrast-filled stomach. Subsequently, "virtual intraluminal endoscopic" views (VIE) of the stomach (Fig. 1 d, 2 c, 3 b, c) were calculated from different vantage points. The VIE software is commercially available from GE Medical Systems (Buc, France). Endoscopic views were rendered using a ray-casting algorithm which selected visible voxels by tracing rays from the current viewing position. The walls (opaque voxels) were identified by a thresholding technique. All pixels above the threshold were considered to be within the gastric lumen.

Three-dimensional intraluminal views of the stomach were rendered at 2-mm steps with a surface mode using a threshold of 300. Each "virtual gastroscopy" consisted of approximately 60 constructed endoscopic views. Each endoscopic image simulated a coned view, the tip of which was located at the observer's position. For a wide FOV, the cone angle was adjusted to 60°. The endoscopic views were displayed with a frame rate of 10/s, and the resulting "virtual gastroscopy" was registered on videotape. The post-processing time for each gastric 3D data set (three sets per patient) was 15 min for a total of 45 min.

Results

Magnetic resonance gastrography was tolerated well by all subjects. In all six subjects the entire stomach was contained within the coronal data sets acquired breath-held over 35 s. Despite the presence of residual air, the entire stomach, from fundus to pylorus, could be fully assessed in all subjects. The 45° left lateral decubitus in conjunction with the supine data set covered all parts of the gastric wall. The duodenal bulb was visualized in the right lateral decubitus position. Post-processing allowed the 3D data sets to be displayed as MIPs, SSDs, and VIEs.

The 3D acquisition did indeed provide a comprehensive endo- and exoscopic analysis of the stomach (Figs. 1–3). Analysis of the source images provided an in-depth understanding of gastric morphology (Figs. 2 a, b, 3 a). This was found to be particularly helpful in the patient with gastric banding, where the interactive use of oblique multiplanar reformations allowed the exact determination of the diameter of the residual lumen narrowed by the gastric band (Fig. 2 a, b). Volumetry of the proximal gastric pouch was possible. The mass lesions of the other two patients were also well visualized (Fig. 3 a): The size of the tumors could be accurately estimated.

Both gastric lesions were easily identified on exoscopic and endoscopic views (Fig. 3). On the virtual gastroscopic images, the regular pattern characterizing the normal mucosa observed in the examined volunteers (Fig. 1 c) could easily be differentiated from the course and irregular pattern characterizing the polypous gastric wall infiltration (Fig. 3 c) in one of the examined patients. The breach of the longitudinal gastric folds by the amorphous surface of the gastric cancer in the third patient was seen on the individual source images as well as on the virtual endoscopic renderings. Delineation of tumor infiltration into the gastric wall was improved following intravenous administration of paramagnetic contrast (Fig. 3 e). The tumor tissue was found to enhance. There was no evidence of local or hepatic metastasis in both cases.

Discussion

Lack of ionizing radiation or other harmful side effects add to the attractiveness of gastric MR imaging. The subjects found the taste of the blueberry-juice-based contrast to be agreeable. Blueberry juice contains manganese and hence causes considerable T1 shortening [12]. To reduce the T1 relaxation time even further, 2 ml of a gadolinium chelate (Gd-DOTA) was added to the 400 ml contrast volume. Gd-DOTA is stable even in an acidic environment [13]. Similar to other Gd-based compounds, it is generally used intravenously and is characterized by a very favorable safety profile even if extravasated [14]. Anaphylactoid reactions are rare [15]. Since only a small amount of paramagnetic contrast is required in addition to the blueberry juice, the contrast mix is inexpensive. Preceding "in vitro" experiments had shown that the sole use of blueberry juice does not provide sufficient T1 shortening. Replacing the blueberry juice with water would require more Gd-DOTA in addition to negatively impacting the taste of the contrast agent.

Magnetic resonance gastrography requires use of only a single liquid contrast making the examination technically less challenging and more comfortable compared with a conventional double-contrast barium study. Similar to conventional gastroscopy, MR gastroscopy requires a clean stomach. The six subjects fulfilled these requirements, having fasted for 4 h prior to the MRI study.

The data for each 3D image set were collected in only 35 s – fast enough to allow data collection in apnea, thereby eliminating respiration-induced motion artifacts. The administration of scopolamine eliminated bowel motion and at the same time permitted adequate distention of the stomach. The 3D technique employs ultrashort TR and TE times. The very short TE limits susceptibility effects caused by air/tissue interfaces. The ultrashort TR in conjunction with a relatively high flip angle minimizes the signal of the abdominal tissues [10]. Against this background, the contrast-filled gastric lumen appears bright and thereby becomes selectively visible (Figs. 1–3). The resultant high quality of the 3D

gastric data sets permitted a comprehensive 3D exo- and endoscopic analysis of all six evaluated stomachs.

The 3D data sets can be viewed in various manners. Multiplanar reformations, providing an in-depth understanding of gastric morphology (Fig. 2 a, b), were available immediately following data acquisition and required no further post-processing. Source images permitted volume calculations of the proximal gastric pouch. The 3D acquisitions also permitted calculation of MIP, SSD, and virtual endoscopic views (Figs. 1–3).

The technique's success is predicated upon the presence of homogeneous contrast within the structure under consideration. The presence of air, found in all evaluated stomachs, can hamper the virtual endoscopic analysis. Air–fluid levels are readily seen on the post-processed images (Fig. 1 b). To assure complete analysis of all portions of the stomach, data sets were acquired in three patient positions. The combination of the 45° left lateral decubitus in conjunction with the supine position was found to cover all parts of the gastric wall in all six subjects. The right lateral decubitus position permitted filling of the duodenal bulb with contrast permitting a virtual endoscopic evaluation of this critical region.

Although "virtual" MR gastroscopy is limited in spatial resolution, these initial results hold promise regarding the ability to permit assessment even of fold patterns (Fig. 1 d). For a thorough assessment of the mucosa, better spatial resolution is definitely required. The implementation of zero filling routines [16] and the use of shorter repetition times will considerably augment spatial resolution in the foreseeable future, without exceeding imaging times beyond a single breathhold. Volume-rendering techniques [17] may further enhance the performance of 3D MR gastroscopy. With volume-rendering voxels exceeding a pre-defined threshold build up one volume, whereas voxels with intensity values below a second threshold form another. The border area of the two volumes will then be displayed on a gray scale, which may enhance the definition of the gastric wall.

The combination 3D gastric MRI with conventional forms of MR imaging enhances its utility (Fig. 3 e). The use of contrast-enhanced dynamically collected multiplanar acquisitions permits local, lymph node, and hepatic staging all within the same examination. Naturally, sequences exploiting the natural T1 and T2 contrast of the MRI experiment may also be added as needed.

A gastric MRI examination can be completed in under 15 min. Post-processing times for 3D data sets, however, are too long. This is more a reflection on the hardware used than on the principle of the technique. Newer hardware with enhanced memory is already available.

Undoubtedly multiple aspects of gastric MR imaging will require improvements and further testing prior to a clinical implementation. We are hopeful that this preliminary report will stimulate other investigators to explore the potential of this new technique.

Acknowledgement. This study was supported by Swiss National Science Foundation, no. 32–045–688.

References

1. Levine MS, Creteur V, Kressel HY, Laufer I, Herlinger H (1987) Benign gastric ulcers: diagnosis and follow-up with double-contrast radiography. Radiology 164: 9–13
2. Keto P, Suoranta H, Ihamaki T, Melartin E (1979) Double contrast examination of the stomach compared with endoscopy. Acta Radiol Diagn 5: 762–768
3. Thoeni RF, Cello JP (1980) A critical look at the accuracy of endoscopy and double-contrast radiography of the upper gastrointestinal (UGI) tract in patients with substantial UGI hemorrhage. Radiology 135 (2): 305–308
4. Ominsky SH, Moss AA (1979) The postoperative stomach: a comparative study of double-contrast barium examinations and endoscopy. Gastrointest Radiol 1: 17–21
5. Martin TR, Vennes JA, Silvis SE, Ansel HJ (1980) A comparison of upper gastrointestinal endoscopy and radiology. J Clin Gastroenterol 2: 21–25
6. Arrowsmith JB, Gerstman BB, Fleischer DE, Benjamin SB (1991) Results from the American Society for Gastrointestinal Endoscopy/U.S. Food and Drug Administration collaborative study on complication rates and drug use during gastrointestinal endoscopy. Gastrointest Endosc 37: 421–427
7. Gonvers J-J, Burnand B, Froehlich F, Pache I, Thorens J, Fried M, Kosecoff J, Vader J-P, Brook RH (1996) Appropriateness and diagnostic yield of upper gastrointestinal endoscopy in an open-access endoscopy unit. Endoscopy 28: 661–666
8. Leung DA, McKinnon GC, Davis CP, Pfammatter T, Krestin GP, Debatin JF (1996) Breath-hold, contrast-enhanced, three-dimensional MR angiography. Radiology 201: 569–571
9. Davis CP, Ladd ME, Romanowski BJ, Wildermuth S, Knoplioch JF, Debatin JF (1996) Human aorta: preliminary results with virtual endoscopy based on three-dimensional MR imaging data sets. Radiology 199: 37–40
10. Luboldt W, Bauerfeind P, Steiner P, Fried M, Krestin GP, Debatin JF (1997) Preliminary assessment of three-dimensional magnetic resonance imaging for various colonic disorders. Lancet 349: 1288–1291
11. Debatin JF, Schoenenberger AW, Luboldt W, Bauernfeind P, Krestin GP (1997) In vivo exoscopic and endoscopic MR imaging of the colon. Am J Roentgenol 169: 1085–1088
12. Hiraishi K, Narabayashi I, Fujita O, Yamamoto K, Sagami A, Hisada Y, Saika Y, Adachi I, Hasegawa H (1995) Blueberry juice: preliminary evaluation as an oral contrast agent in gastrointestinal MR imaging. Radiology 194: 119–123
13. Schwizer W, Fraser R, Maecke H, Siebold K, Funck R, Fried M (1994) Gd-DOTA as a gastrointestinal contrast agent for gastric emptying measurements with MRI. Magn Reson Med 31: 388–393
14. Cohan RH, Leder RA, Herzberg AJ, Hedlund LW, Wheeler CT, Beam CA, Nadel SN, Dunnick NR (1991) Extravascular toxicity of two magnetic resonance contrast agents. Preliminary experience in the rat. Invest Radiol 26: 224–226
15. Weiss KL (1990) Severe anaphylactoid reaction after i.v. Gd-DTPA. Magn Reson Imaging 8: 817–818
16. Korosec FR, Frayne R, Grist TM, Mistretta CA (1996) Time-resolved contrast-enhanced 3D MR angiography. Magn Reson Med 36: 345–351
17. Rubin GD, Beaulieu CF, Argiro V, Ringl H, Norbash AM, Feller JF, Dake MD, Jeffrey RB, Napel S (1996) Perspective volume rendering of CT and MR images: applications for endoscopic imaging. Radiology 199: 321–330